

## Effect of CoO on the Formation of Mullite Ceramics from Diphasic Al<sub>2</sub>O<sub>3</sub>-SiO<sub>2</sub> Gel

J. Roy<sup>1</sup>, N. Bandyopadhyay<sup>2</sup>, S. Das<sup>3</sup> and S. Maitra<sup>\*4</sup>

<sup>1</sup>Camellia Institute of Technology, Badu, Madhyamgram, Kokata-700127, India.

<sup>2</sup>Govt. College of Engineering and Ceramic Technology, 73, A. C. Banerjee Lane, Kolkata-700010, India.

<sup>3</sup>Mechanical and Metallurgical Engineering, Florida International University, USA.

<sup>4</sup>Universiti Teknologi PETRONAS, Tronoh-31750, Perak, Malaysia.

Received 12 October 2009; Revised 19 April 2010; Accepted 21 June 2010

### Abstract

In this work the effect of CoO additive on the formation of mullite from Al<sub>2</sub>O<sub>3</sub>-SiO<sub>2</sub> diphasic gel has been studied. The diphasic gel precursor for mullite was synthesized by sol-gel route following aqueous phase colloidal interaction of aluminium hydroxide and silicic acid. The precursor gel powder was thoroughly characterized by chemical analysis, measurement of surface area, bulk density and also by FTIR spectroscopic studies. The gel powder was compacted with the CoO additives in different ratios and sintered at three different elevated temperatures. Microstructure of the sintered compacts was analyzed from SEM studies and phase analyses were carried out from XRD studies. It has been observed that the morphology of the mullite crystals changed significantly in the presence of the additives. As a result of the inclusion of additive maximum expansion in the b-axis of the mullite crystal took place. With the addition of 3% additive more than 14% mullite formation occurred after sintering. A significant improvement in the formation of mullite in the sintered masses was also observed in the presence of CoO additive. More than 10% improvement in density as well as flexural strength and about 5% improvement in fracture toughness of the sintered compacts were observed in the presence of the CoO additive.

*Keywords:* Mullite, Di-Phasic gel, CoO additive, Mechanical properties, Microstructure.

### 1. Introduction

Mullite has achieved considerable importance as an engineering material for its several remarkable physico-chemical properties. These properties include low thermal expansion and thermal conductivity, good thermal and chemical stability, high melting point, low creep rate, reasonable toughness and strength, good thermal shock resistance, adequate infrared transparency etc [1-4]. For these beneficial properties mullite ceramics are widely used in the production of heat resistant materials in heat insulation, refractories, heat exchanger, turbine blades, spacecraft components, computer chips etc. [5, 6]. Composition wise mullite is basically a non-stoichiometric compound and its molecular formula can be represented as Al<sub>2</sub>[Al<sub>2+2x</sub>Si<sub>2-2x</sub>]O<sub>10-x</sub>, where x denotes the number of missing oxygen and atoms per unit cell, varying between 0.25 and 0.59 [7, 8]. Although there have been different methods existing for the synthesis of mullite, during the last few years chemically synthesized active precursors have been widely employed for the processing of mullite. These precursors are converted to mullite at a relatively low temperature range from ~850° to ~1350°C [9-11] and this type of mullite is known as “chemical mullite” [12]. Among several methods, sol-gel process is one of the widely used

processes for the synthesis of chemical mullite. By sol-gel process generally three sequences for mullite crystallization may be observed [13], (i) mullite may be crystallized from the amorphous phase directly for single phase gel (ii) mullite can be crystallized via spinel phase (iii) mullite also can be crystallized from the reaction of discrete crystalline or semicrystalline alumina and amorphous silica from diphasic gels. Researchers have been focusing on the diphasic gel precursors for its relatively higher activity for the synthesis of advanced materials. Diphasic gels as type-II precursors of mullite [14] consist of pseudo boehmite and amorphous silica at room temperature. During heat treatment boehmite forms δ-Al<sub>2</sub>O<sub>3</sub>, this reacts with amorphous silica to form mullite above 1250°C. Type-III diphasic gel are non-crystalline up to 980°C and mullite formation is preceded by the formation of a weak crystalline transient alumina such as cubic Al-Si spinel or γ-Al<sub>2</sub>O<sub>3</sub> at 980°C, which later reacts with amorphous silica to form mullite at < 1250°C.

Different transition metal oxides have been shown to have favourable mineralizing effect on the formation of mullite ceramics from the precursor materials. Ferriera da Silva [15] observed that presence of manganese ion can induce mullitization at lower temperature from Al<sub>2</sub>O<sub>3</sub>-SiO<sub>2</sub> gel. Martisius and Giraitis [16] ob-

\* E-mail address: drsaiikat\_maitra@petronas.com.my

ISSN: 1791-2377 © 2010 Kavala Institute of Technology. All rights reserved.

served that copper oxide as an additive can decrease the transformation temperature of kaolinite to mullite by 200°C. Kong et al [17] observed that  $V_2O_5$  accelerated the mullite phase formation, while  $Nb_2O_5$  and  $Ta_2O_5$  inhibited the mullitization. Baudin and Moya [18] investigated the influence of  $TiO_2$  on the sintering and microstructural evolution of mullite and observed that addition of  $TiO_2$  under the solubility limit enhanced the initial sintering and grain size in mullite whereas an amount in excess of that limit inhibit sintering and drastically increased the total porosity and mean pore size. Nass et al [19] studied on the influence of chromium ion on homogeneity of gels and on mullite formation at 980°C by DTA coupled with quadrupole mass spectrometry, SEM, EDX and TEM analysis and observed that the difference in chromium content affected significantly the crystallization path of mullite. Mitra et al [20] also observed that  $Cr_2O_3$  played a positive role in the formation of mullite at elevated temperatures from the aluminosilicate gel precursor. Some workers used copper oxide as additive for reducing the formation temperature for the conversion of kaolinite to mullite [21, 22]. Schneider and Vasudevan [23] worked on manganese doped mullites synthesized from metal organic starting materials by a modified sol-gel technique at low temperature and suggested that up to ca 6wt%  $Mn_2O_3$  can enter the mullite structure. Dayal et al [24] determined the free energy value for the formation of mullite as -5.8 kCal at 1422°C from the oxide components under equilibrium condition in the system  $CoO-Al_2O_3-SiO_2$ . Schneider [25] observed that cobalt doped mullite produced electron paramagnetic resonance (EPR) spectra with signals near  $g_{eff} = 4.9$  and 2.2.

In the present investigation the effect of CoO on the crystallization of mullite from  $Al_2O_3-SiO_2$  bi-phasic gel precursor powder derived from inorganic salts was investigated by analyzing the microstructure and mechanical properties of sintered products.

## 2. Experimental

The aluminosilicate hydrogel was synthesized from the starting materials  $Al(NO_3)_3 \cdot 9H_2O$  (analar grade) and liquid sodium silicate (analar grade with sp. Gr. 1.6 and molar ratio of  $Na_2O: SiO_2 = 1:3$ ) Chemical compositions of the starting materials is given in table 1. Silicic acid was prepared by ion exchange process from sodium silicate using Dowex-50 cation exchanging resin in a column exchanger. 7% (w/v) sodium silicate solution was used as the feed with a flow rate of 200 ml/minute. Silica sol was prepared by ultrasonic dispersion of the generated silicic acid (5% w/v) in aqueous phase. The silica sol formed was mixed with 10% (w/v)  $Al(NO_3)_3 \cdot 9H_2O$  solution stoichiometrically to attain a molar ratio close to 3:2 ( $x=1/4$ ) for  $Al_2O_3$  and  $SiO_2$  in the mix at pH=2. To the mixed solution 1:1 ammonia solution was added slowly with stirring till a neutral pH was attained. The mixed sol was allowed to age to form the gel. The gel was filtered, washed thoroughly, dried at 80°C and characterized by chemical analysis, measurement of surface area and bulk density. The results are given in table 2. The gel was calcined at 800°C for a period of 2 hours. The calcined gel was properly pulverized in a pot mill and thoroughly mixed with CoO (Reagent Grade) additive in different ratios by co-grinding. The composition of the different batches is given in table 3. The powder mixes were compacted at 100 MPa. The samples were

fired in an electrically heated muffle furnace at three different final temperatures, ca., 1400, 1500 and 1600°C, with 2 hours of soaking period in each case. Bulk density and apparent porosity of the sintered samples were measured following the procedures described in BS 1902, Part 1A, 1966. The flexural strength of the sintered samples were determined from a three point bending strength with a span of 30mm and a loading rate of 0.5 mm/min. Fracture toughness was determined by using an indentation micro-crack method with a load of 5 kg. [26]. XRD pattern of the samples was taken with a Rigaku X-ray diffractometer with Cu target (Miniflex, Japan). Scanning electron microscopic investigation of the samples was carried with FEI Quanta microscope (US).

## 3. Results and Discussion

Silica sol is a positively charged colloid and after generation by ion exchange process, it did not show any tendency of polymerization. When silica sol was mixed with  $Al(NO_3)_3$  solution, the solution became acidic. With the addition of ammonium hydroxide non-simultaneous formation of the aluminium hydroxide and polysilicic acid gels took place and therefore, the formed aluminosilicate gel was bi-phasic in nature. In this system discrete aluminum hydroxide gel particles were likely to be distributed uniformly in the high molecular weight polysilicic acid gel network.

**Table 1.** Chemical constituents of the ingredients (wt %).

Ingredients	$SiO_2$	$Al_2O_3$	$Na_2O$
Sodium silicate	29.75	-	17.41
Aluminium nitrate	-	12.98	-
Batch composition	27	73	-

**Table 2.** Physicochemical properties of the hydrogel.

Composition	Properties
$SiO_2$ (wt %)	17.86
$Al_2O_3$ (wt %)	48.23
Ignition Loss (wt %)	33.91
Bulk density ( $g/cm^3$ )	0.27
Sp. Surface area ( $m^2/g$ )	170

**Table 3.** Batch composition of the samples.

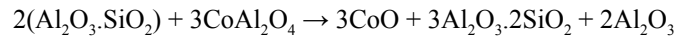
Batch No.	$Al_2O_3-SiO_2$ Hydrogel	CoO
1	100	0
2	99	1
3	98	2
4	97	3

The precursor gel powder is expected to have considerable surface activity as it had a very low bulk density ( $0.27g/cm^3$ ) and

a considerably high surface area (70m<sup>2</sup>/gm). As the hydro-gel contained significant amount of water (33.91%) it was calcined at 800°C to prevent excessive shrinkage during sintering. The composition of the aluminosilicate was intentionally kept slightly in the alumina rich zone of the mullite (molar ratio of Al<sub>2</sub>O<sub>3</sub>/SiO<sub>2</sub> 3.18) to minimize the formation of glassy phase after sintering. After synthesis no deviation was observed from the parent batch composition in the synthesized material as in the alumina rich zone all of the silica in the composition was likely to get converted to mullite phase.

In the FT-IR spectra of the gel sample (Figure 1) the peaks at 3464 cm<sup>-1</sup> and 1637cm<sup>-1</sup> were assigned to the stretching and bending mode of adsorbed water since the precursor gel was prepared under basic condition where the gelation occurred rapidly. The Al(OH)<sub>3</sub> was precipitated out in colloidal form along with precipitates of Si(OH)<sub>4</sub> and they grew rapidly side by side to form diphasic gel [27]. The band at 3151cm<sup>-1</sup> was assigned to the OH stretching mode of these hydroxides. Corresponding OH bending vibration was observed at 1105.7cm<sup>-1</sup>, which overlapped with the stretching vibration of Si-O-Si of the gel network. The sharp peak at 1388.4 cm<sup>-1</sup> indicated the presence of trace amount of nitrate from the starting material aluminium nitrate in the gel structure [28]. The stretching modes of Al-O-Al linkages were observed at 618.7 and 747.7 cm<sup>-1</sup>. The band at 477.9 cm<sup>-1</sup> was assigned to Si-O stretching vibration. No characteristic band for Si-O-Al linkage was observed, which suggested that the precursor maintained true diphasic gel characteristics. Mullite formation in diphasic aluminosilicate gel is controlled by dissolution-precipitation reactions, where Al<sub>2</sub>O<sub>3</sub> species dissolve in the co-existing SiO<sub>2</sub> liquid until a critical Al<sub>2</sub>O<sub>3</sub> concentration is reached [28, 29]. Al<sub>2</sub>O<sub>3</sub> particles act as the nucleus for mullite formation and higher Al<sub>2</sub>O<sub>3</sub> concentrations can induce random mullite nucleation in the bulk of the SiO<sub>2</sub>-rich phase. Therefore, the dissolution velocity of Al<sub>2</sub>O<sub>3</sub> into the SiO<sub>2</sub> liquid is the rate limiting step for the nucleation and subsequently growth of mullite crystals.

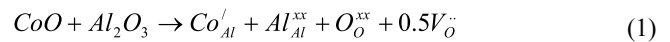
The additive CoO used in the present investigation has a periclase (rock salt) structure with a lattice constant of 4.2615 Å [30]. According to CoO-Al<sub>2</sub>O<sub>3</sub>-SiO<sub>2</sub> phase diagram, within the compositional range selected in the present investigation, cobalt silicate and cobalt spinel (cobalt aluminate) are likely to form in the presence of CoO. In the presence of excess Al<sub>2</sub>O<sub>3</sub> and SiO<sub>2</sub> cobalt silicate and cobalt aluminate is converted to thermodynamically more stable mullite in the following way,



In other words, CoO reduces the energy barrier for the formation of mullite via the intermediate formation of active cobalt silicate and cobalt aluminate. The presence of cobalt silicate and cobalt aluminate was also detected by XRD studies.

Again, the 3d<sup>7</sup> electrons of Co<sup>2+</sup> in an octahedral crystal field are split from the energetic ground state to the low spin state (t<sub>2g</sub>)<sup>6</sup>(e<sub>g</sub>)<sup>1</sup>. The e<sub>g</sub> electron occupies the d<sub>z<sup>2</sup></sub> orbital and not the d<sub>x<sup>2</sup>-y<sup>2</sup></sub> orbital. The d<sub>z<sup>2</sup></sub> electron can repel the electrons of the respective oxygen ligands. As a result the octahedron's z-axis is lengthened. Therefore a deformation in oxygen octahedral takes place. This distortion is known as Jahn-Teller distortion [31]. Moreover the cationic size of six-coordinated Co<sup>2+</sup> under low spin state is 83.8 pm [32] which is larger than that of Al<sup>3+</sup>[53pm]. Therefore mullite lattice undergoes deformation lattice deformation in the presence of Co<sup>2+</sup>. This deformation is responsible for expansion of lattice along b-axis and shortening along a-axis. Earlier studies also indicated that Co<sup>2+</sup> existed in octahedral coordination in mullite structure [25].

The incorporation of Cobalt (II) ions into the aluminosilicate samples also can induce defect in the structure in the following way,



The defect generated can assist in further densification of the material during heat treatment.

Formation of both cobalt silicate and cobalt aluminate phases was observed from the XRD diffractogram of the samples (Figures 2A and 2B). The lattice parameters of the doped and undoped mullite crystals were calculated following the process as described by Krishna Murthy and Hummel [33]. The calculated values of lattice parameters of undoped mullite were like the following, a=7.5238Å, b=7.6789Å and c=2.8671Å with lattice volume of 165.65(Å)<sup>3</sup>. For the sample with 3% CoO the lattice parameters were like the following, a= 7.5321Å, b=7.7314Å and c = 2.8892Å with cell volume 168.24 (Å)<sup>3</sup>. Therefore a volume expansion of about 1.56% took place for mullite crystal as a result of doping with 3% CoO. From the cell parameters it was observed that the maximum deviation took place along the b-axis of the crystallite. Again the relative percentage of mullite also increased with the increase in the both CoO content and sintering temperature. The mullite content in different batches was estimated using XRD technique following the procedure described by Chung [34]. It was observed that with the addition of 3% CoO about 14.5% more mullitization was achieved at the highest sintering temperature of 1600°C (Figure 2C).

Grain size of the sintered mullite samples were calculated from the XRD profiles using Scherrer's equation. In this case it has been assumed that both stress and particle size leads to size broadening of the diffraction peaks. Instrumental contribution was also taken into consideration for peak broadening [35, 36]. The modified Scherrer's equation as given below has been used for this purpose.

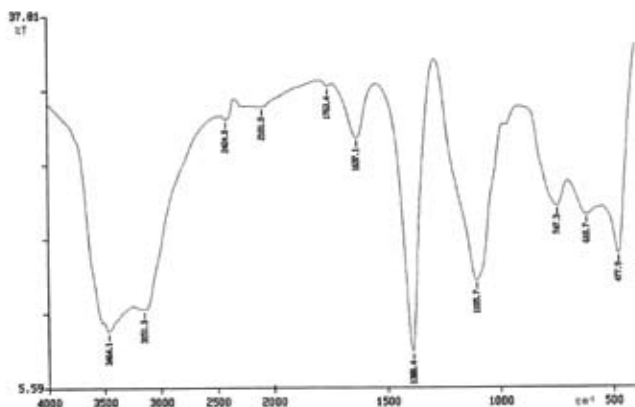


Figure 1. FT-IR Spectra of The Gel Sample

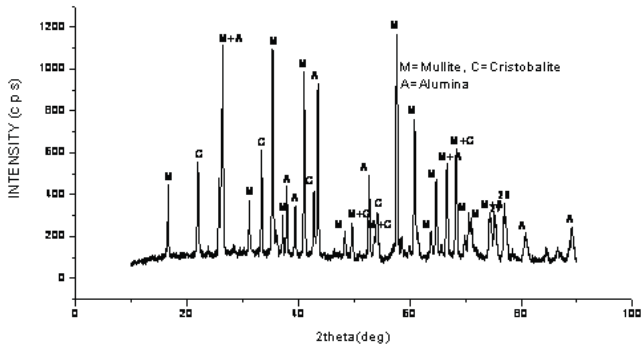


Figure 2A. XRD Diagram of the gel (no additive) sintered at 1500°C

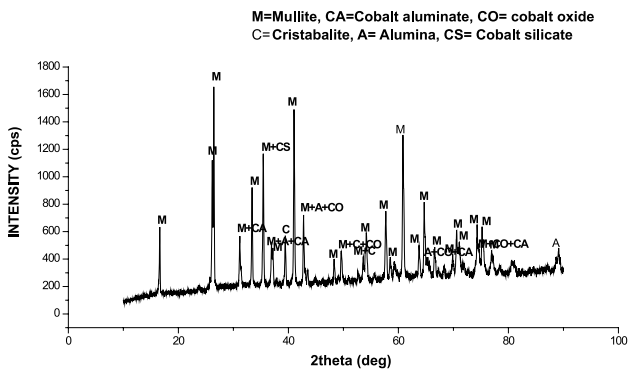


Figure 2B. XRD Diagram of the sintered gel with 3% Cobalt Oxide at 1500°C

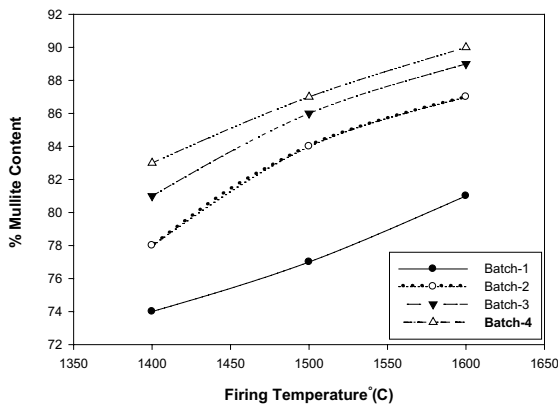


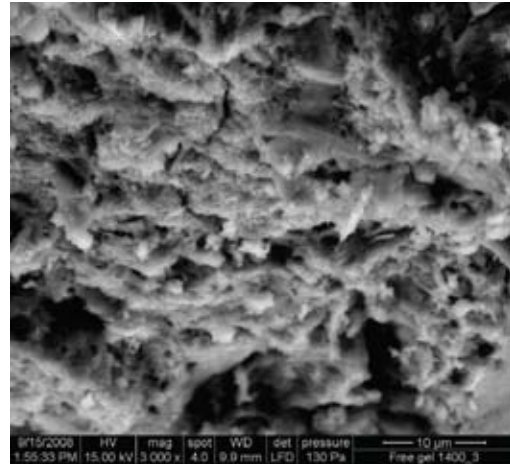
Figure 2C. Variation in Mullite Content with Firing Temperature

$$\beta_i^2 = \left( \frac{0.9\lambda}{D \cos\theta} \right)^2 + (4\varepsilon \tan\theta)^2 + \beta_0^2 \quad (2)$$

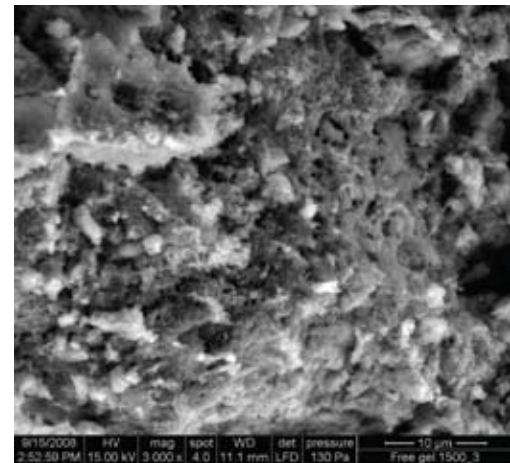
$\beta_i$  represents total broadening,  $\varepsilon$  is the strain,  $\lambda$  is the wavelength,  $\theta$  is the diffraction angle.  $\beta_0$  is the instrumental broadening,  $D$  is the average particle size. By a least square method the experimentally observed broadening of several peaks were used to compute the average particle size  $D$  and the strain  $\varepsilon$  simultaneously.

The average crystallite size calculated for sample with 3% CoO content was found to be 4.4  $\mu\text{m}$  at a sintering temperature of 1400°C, 3.5  $\mu\text{m}$  at a sintering temperature of 1500°C and 1.9  $\mu\text{m}$  at a sintering temperature of 1600°C. The corresponding values of average microstrains were 0.0028 at 1400°C, 0.0017 at 1500°C and 0.0008 and 1600°C respectively.

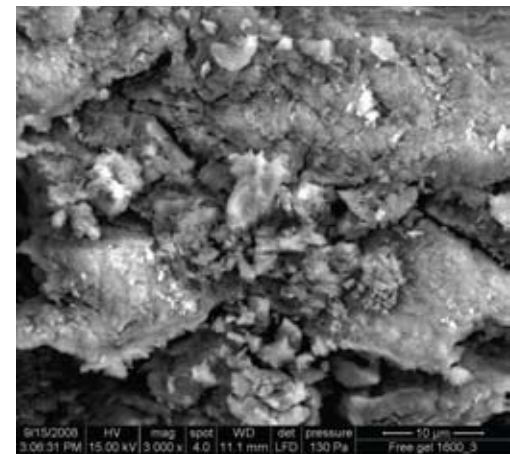
From the SEM micrographs of the sintered samples (Figures 3A and 3B) it is apparent that un-doped sol-gel mullite formed very small crystallites. The incorporation of cobalt ions in the sol-gel mullite induced tabular crystal growth parallel to the crystallographic c-axis. With the increase in the cobalt ion content in mullite, formation of more equi-axed but smaller sized crystallites was observed. With the increase in the sintering temperature also the size of the crystallites reduced. The microstructure became more cohesive with the increase in the additive content.



(i)



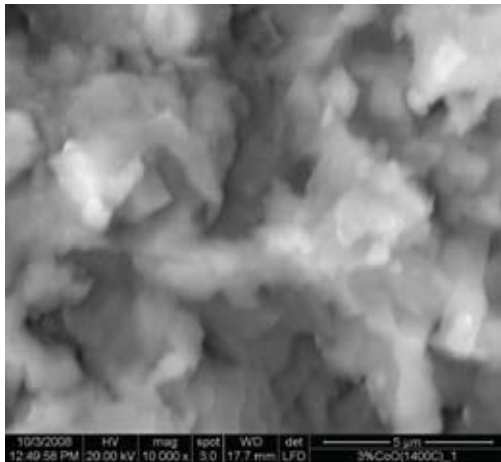
(ii)



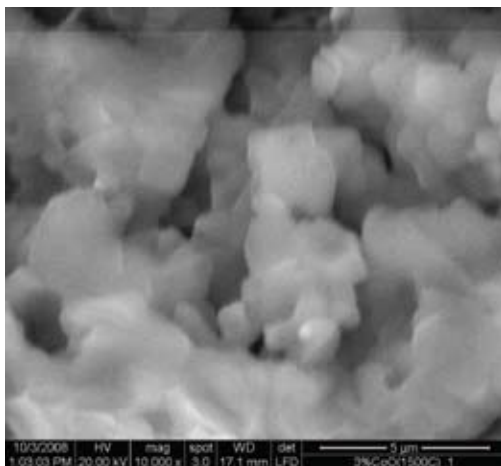
(iii)

Figure 3A. Scanning Electron Micrograph of the sintered gel samples (no additive) (i): sintered at 1400°C (ii) sintered at 1500°C (iii) sintered at 1600°C

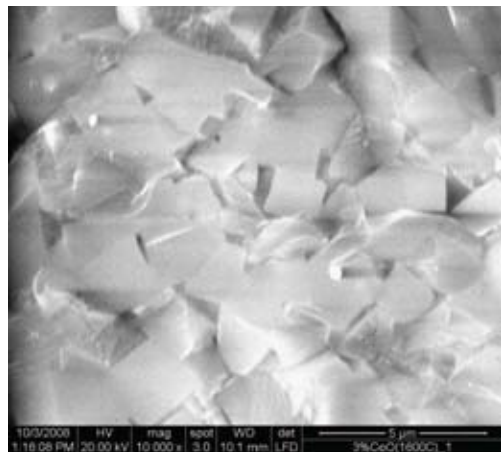
The variation in bulk density and apparent porosity (Figures 4 and 5) of the samples with sintering temperature has been shown in figures 3 and 4. From the figures it is clear that CoO exhibited a positive effect on the densification of the mullite ceramics. About 15% improvement in the density was observed with 3% CoO content at the highest sintering temperature under the investigation. The apparent porosity was reduced by 35% in the presence of 3% additive at the sintering temperature of 1500°C.



(i)



(ii)



(iii)

Figure 3B. Scanning Electron Micrograph of the sintered gel samples with 3% cobalt oxide additive(i): sintered at 1400°C (ii) sintered at 1500°C (iii) sintered at 1600°C

The flexural strength and fracture toughness (Figures 6 and 7) of the samples also increased in the presence of CoO additive. It can be related to the development of interlocked elongated crystal in the microstructure. The grain boundary did not contain noticeable glassy phases. The effect was more pronounced for the batch containing 2% additive. The flexural strength increased by 13% with the addition of 2% additive at a sintering temperature of 1500°C. Similarly the fracture toughness of the samples was also improved in the presence of CoO additive. Fracture toughness increased by about 5% with the addition of 3% additive at the sintering temperature of 1600°C. A small amount of highly viscous silica or aluminosilicate glass can exist at the grain boundaries, which would minimize the contribution of grain boundary sliding to the fracture stress [37].

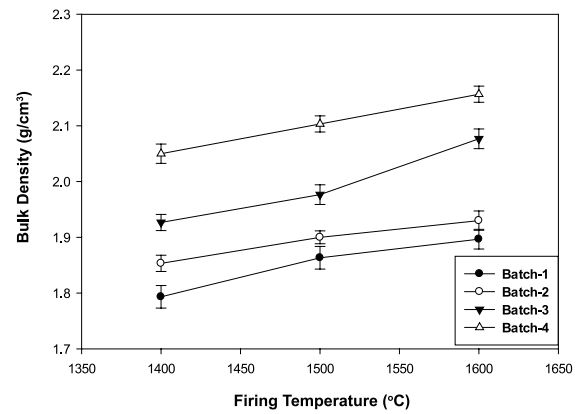


Figure 4. Variation in Bulk Density with Firing Temperature

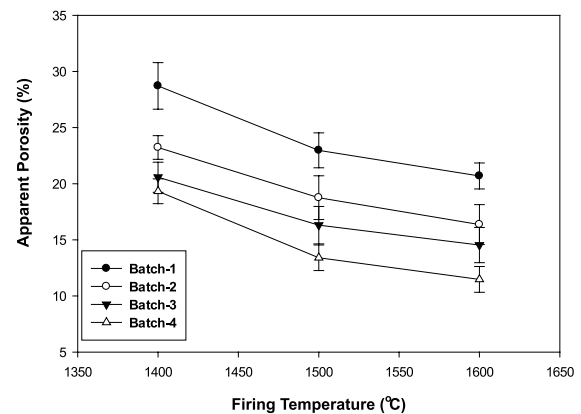


Figure 5. Variation in Apparent Porosity with Firing Temperature

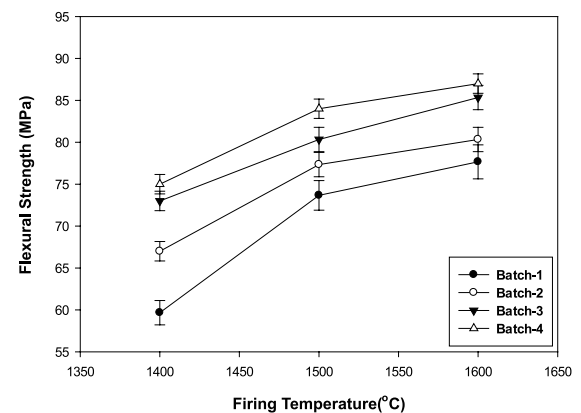


Figure 6. Variation in Flexural Strength with Firing Temperature

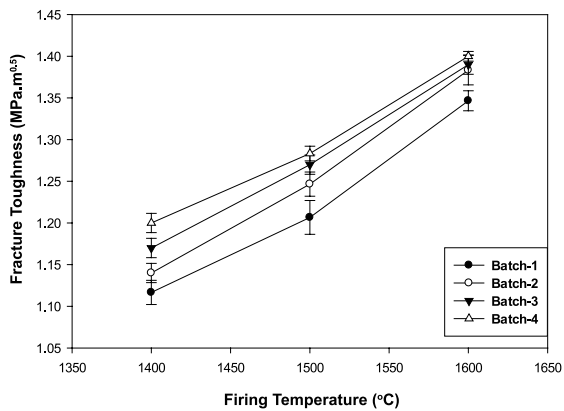


Figure 7. Variation in Fracture with Firing Temperature

#### 4. Summary and Conclusion

Mullite ceramics was synthesized from the biphasic aluminosilicate gel precursor, which was prepared by the colloidal interaction of silicic acid and  $\text{Al}(\text{NO}_3)_3$  solution. The gel powder possessed very low density and high surface area and consisted of separate non-linked units of alumina and silica gel. CoO was used as sintering additive for the processing of mullite ceramics in different proportions. CoO promoted the formation of mullite by the interaction between  $\text{Al}_2\text{O}_3$  and  $\text{SiO}_2$  via the intermediate formation of cobalt silicate and cobalt aluminate. Different mechanisms like, interaction with the alumina and silica sub lattices, Jahn-Teller effect, anionic vacancy formation of liquid phase at higher temperature etc. was put forward to explain the favourable effect of CoO. The crystallite size of mullite was also modified by CoO. The mechanical properties of the sintered masses were also improved significantly due to improved microstructure and favourable phase compositions.

#### References

- W. Kollenberg, H. Schneider, *J. Am. Ceram. Soc.*, **72**, 1739 (1989).
- A. P. Hynes, R. H. Doremus, *J. Am. Ceram. Soc.*, **74**, 2469 (1991).
- A. Aksay, D. M. Dabbs, M. Sarikaya, *J. Am. Ceram. Soc.*, **74**, 2343 (1991).
- H. Schneider, E. Eberhard, *J. Am. Ceram. Soc.*, **73**, 2073 (1990).
- B. Kanka, H. Schneider, *J. Mater. Sci.*, **29**, 1239 (1994).
- M. Sarikaya, I. A. Aksay, *J. Am. Ceram. Soc.*, **70**, 837 (1987).
- W. E. Cameron, *Am Miner.*, **62**, 747 (1977).
- D. J. Duval, S. H. Risbud and J. F. Shackelford, *Ceramics and Glass Materials: Structure, Properties and Processing*, eds. J. F. Shackelford and R. H. Doremus, Springer (2008).
- B. E. Yoldas, *Am. Ceram. Soc. Bull.*, **59**, 479 (1980).
- W. Hoffman, R. Roy, S. Komarneni, *J. Am. Ceram. Soc.*, **69**, 468 (1984).
- K. Okada, N. Otsuka, *J. Am. Ceram. Soc.*, **69**, 652 (1986).
- H. Schneider, K. Okada, *J. Pask, Mullite and Mullite Ceramics*, John Wiley and Sons Ltd, England (1994).
- E. Tkalcec, H. Ivankovic, R. Nass, H. Schmidt, *J. Eu. Ceram. Soc.*, **23**, 1465 (2003).
- H. Schneider, D. Voll, B. Saruhan, J. Sanz, G. Schradar, C. Ruscher and A. Mosset, *J. Non Cryst. Sol.*, **78**, 262 (1994).
- M. G. Ferriera da Silva, *J. Sol Gel Sci. Tech.*, **13**, 987 (1998).
- T. Martisius, R. Giraitis, *J. Mater. Chem.*, **13**, 121 (2002).
- L. B. Kong, Y. B. Gan, J. Ma, T. S. Zhang, F. Boey, R. F. Zhang, *J. Alloys Compd.*, **351**, 264 (2003).
- C. Baudin, J. S. Moya, *J. Am. Ceram. Soc.*, **67**, C134 (1984).
- R. Nass, E. Tkalcec, H. Ivankovic, *J. Am. Ceram. Soc.*, **78**, 3097 (1995).
- N. K. Mitra, S. Maitra, D. Gnanabharathi, T. K. Parya, R. Dey, *Ceram. Int.*, **27**, 277 (2001).
- A. A. Spokauskas, P. V. Kicas, *Sbornik Trudov*, **12**, 136 (1979) (in Russian).
- M. Bartsch, B. Saruhan, M. Schmucker, H. Schneider, *J. Am. Ceram. Soc.*, **82** 1388 (1999).
- H. Schneider and R. Vasudevan, *N. Jb. Min. Mh*, **4**, 165 (1989).
- R. R. Dayal, R. E. Johnston and A. Muan, *J. Am. Ceram. Soc.*, **50** (10), 537 (2006).
- H. Schneider, *Ceram. Trans.*, **6**, 135 (1990).
- D. J. Janackovic, V. Jakanovic, L. J. Kostic-Gvozdenovic, D. Uskokovic, *Nanostruct Mater*, **10**(3), 341 (1998).
- R. L. Orfice, W. L. Vasconcelos, *J. Sol-Gel Sci Tech.*, **9**, 239 (1997).
- M. D Sacks, N. Bozkurt, G. W. Scheiffele, *J. Am. Ceram. Soc.*, **74**, 2428 (1991).
- B. de la Lastra, C. Leblud, A. Leriche, F. Cambier, M. R. Anseau, *J. Mater. Sci. Lett.*, **4**, 1099 (1985).
- R. Kannan and M. S. Seehra, *Phys. Rev.* **B35**, 6847 (1987).
- H. Jahn, E. Teller, *Proc. Royal Soc. London. Ser. A, Math. Phys. Sci.* (1934-1990) **161** (905), (1937), 220-235.
- R. D. Shanon, *Acta Crystall*, **A32**, 751 (1976).
- M. Krishna Murthy, F. A. Hummel, *J. Am. Ceram. Soc.* **43**(6), 267 (1960).
- F. H. Chung, *Adv. X-ray. Anal.* **17**, 106 (1973).
- J. I. Langford, *J. Appl. Cryst.*, **11**, 10 (1978).
- J. I. Langford, in: R. L. Snyder, J. Fiala and H. J. Bunge (Eds.), *Defect and microstructure analysis by diffraction*, IUCr Monographs on Crystallography 10, International Union of Crystallography-Oxford Science Publications, New York (1999).
- S. Gupta, M. Dubikova, D. French, V. Sahajwalla, *Energy & Fuels*, **21**, 1052 (2007).